18th International Conference of
Adaptive Structures and Technologies
October 3rd, 4th, 5th, 2007
Ottawa, Ontario, Canada

Experimental validation of the 3D numerical model for an adaptive laminar wing with flexible extrados

D. Coutu, V. Brailovski*, P. Terriault, and C. Fischer
Department of Mechanical Engineering, École de technologie supérieure,
* Corresponding author: 1100 Notre-Dame St. West, Montreal, Canada, H3C 1K3
Tel: 1 (514) 396-8594, Fax: 1 (514) 396-8530, E-mail: vladimir.brailovski@etsmtl.ca

ABSTRACT

Wing drag reduction poses a real challenge in aerospace engineering. At the subsonic speed level, drag reduction can be achieved by increasing laminar flow over the wing. This work focuses on the development and validation of the numerical model of an experimental adaptive wing with improved laminar flow. The wing is composed of a rigid structure forming intrados and wing-box, flexible extrados and actuators located inside the wing-box. The extrados profile is controlled by two individually controlled actuators placed along the wing chord and acting normally to the chord. The flexible extrados is made of a woven carbon/Kevlar hybrid composite designed to allow greater flexural compliance in the chord-wise than in the span-wise direction. To allow the subsequent optimisation of the adaptive wing structure, a structural shell model of the flexible extrados is built using the ANSYS finite element software. The model takes into account the following variables: (1) reinforcement type, properties and stacking sequence, (2) laminate thickness and curvature radius, (3) boundary conditions representing the interaction between flexible and rigid wing structures, and (4) extrados-actuator coupling conditions (location, direction, force and stroke). An adaptive wing prototype has been built to verify the predicted structural response. The experimental validation of the structural model is performed using tensile and three-point bending tests followed by testing of the entire wing structure with a laboratory experimental bench.

Keywords: laminar adaptive wing, drag reduction, 3D finite element modeling, hybrid composite

1. INTRODUCTION

Drag reduction over an airfoil poses a real challenge that has attracted significant attention in the aerospace research community. Up until now, the literature has included discussions of two main methods used for altering the flow dynamics over an airfoil: energizing of the boundary layer [1] and modifying the airfoil profile [2-5]. The second approach partially realized in the works of Chandrasekhara et al [3], Baron et al [4] and Munday et al [5] modifies respectively the leading edge, intrados or extrados of an airfoil to extend the flight envelope, increase lift and avoid laminar flow separation. This work aims to delay the backward transition between laminar and turbulent flow over the airfoil profile using flexible skin partially covering the airfoil extrados. To optimize the design of this flexible skin, which is made of a laminate composite material, the finite element modeling (FEM) approach is used. The adaptive wing with improved laminar flow is composed of the rigid structure① forming intrados and wing-box, the flexible extrados②, the compensation cantilever spring③ and the actuators④ located inside the wing-box, as presented in figure 1.

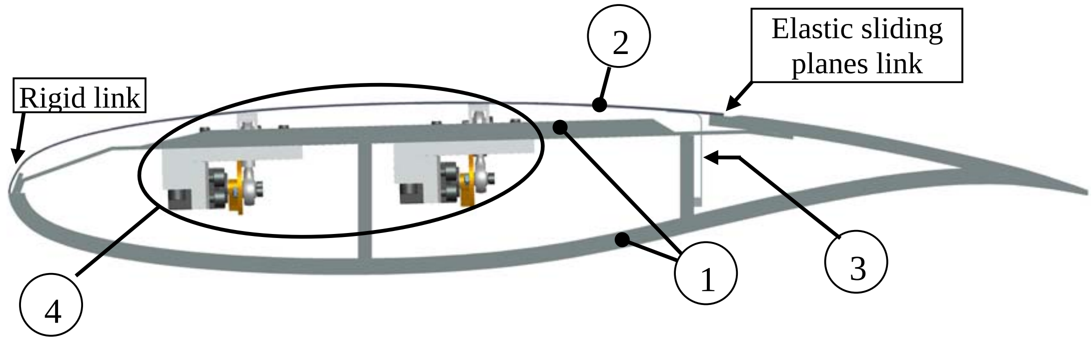

Figure 1. Conceptual design of an improved laminar flow adaptive wing using flexible extrados

To resist potentially high aerodynamic forces, the leading edge of the flexible extrados is firmly attached to the rigid structure. The other extremity of the flexible extrados is linked to a compensation cantilever spring that creates an elastic joint to accommodate extrados shaping and to maintain aerodynamic continuity between the flexible and rigid parts of the wing.

Three main objectives must be taken into account in designing the flexible extrados:

1. The wing profile should be modified according to CFD optimization calculations while maintaining uniformity of the span-wise shape changes.
2. The flexible extrados should be attached to the rigid wing-box structure such as to compensate for geometry variations, while ensuring aerodynamic continuity.
3. The flexible extrados should be connected to the actuators in a manner ensuring global shape modifications.

These general design objectives can be translated into the following technological objectives:

1. The material used to manufacture the extrados should allow the precise control of its structure and properties. In this respect, a laminate composite material is the best solution because it can be tailored to suit each task by varying the stacking sequence, the orientation, and the in-plane extent of the composite reinforcement; the material can then be adapted for a compliant structure that needs to exhibit specific shape changes under actuation.
2. Ultimately, both the material and the technology used to process it may be approved in accordance with existing standards for aviation materials and processes.

Given these premises, finite element modeling (FEM) can assist in the design of the flexible extrados because it allows the designer to predict flexible extrados shape variations based on loading and boundary conditions. Also, the laminate structure can be optimized in order to meet the following performance criteria: (a) conformity of the modified wing geometry with the theoretical profiles resulting from CFD calculations, and (b) compactness and lightness. This paper thus discusses the validation of the finite element model built to assist in the realization of the adaptive wing with improved laminar flow using a flexible extrados.

2. FEM OF THE FLEXIBLE EXTRADOS

ANSYS, commercial finite element analysis software, is used to build a 3D numerical model of the flexible extrados. For validation purposes, the flexible extrados is encompassed between 1 and 64% of a 500 mm length chord constant profile, and forms a 410 mm span wing (figure 2).

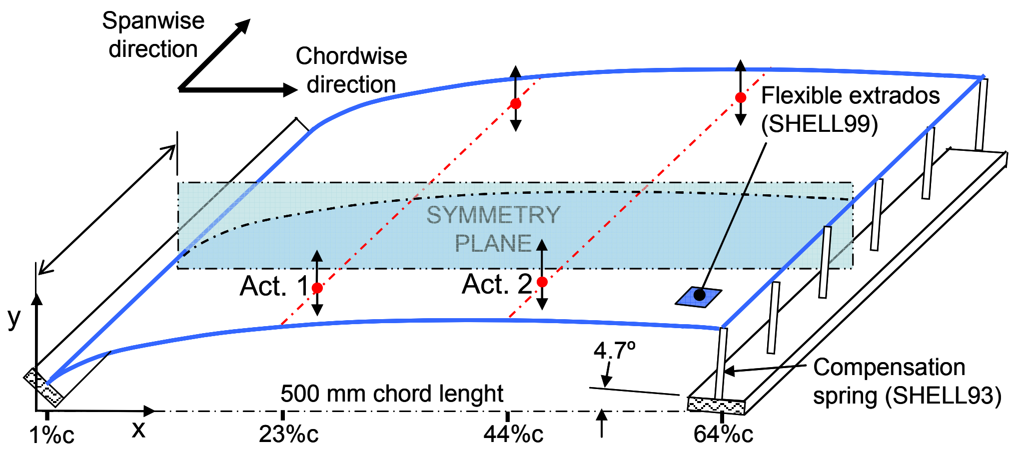

Figure 2. Flexible extrados schematics with boundary and loading conditions

Using symmetry conditions, a 205 mm half span is modeled using Shell99 elements. This 8-node layered structural shell models the laminate made from a series of plies with orthotropic material properties. Furthermore, 3 cantilever springs are modeled at the right end of the extrados using 8-node Shell93 elements to represent an elastic link between the flexible and rigid extrados parts. Actuation forces are distributed over 9.5mm x 19mm rectangular areas representing connection zones between the actuators and the flexible structure. The definitions and properties of each ply are presented in the following section.

The flexible extrados structure is modeled through mapped meshing. To perform a convergence study, 10mm displacement is applied to the structure at a distance corresponding to 23% of the chord length for different mesh densities. For each analysis, the reaction force is reported in respect to the number of element (figure 3). A 1716 quadrilateral elements mesh is the best compromise between CPU time calculation and results accuracy for subsequent analyses.

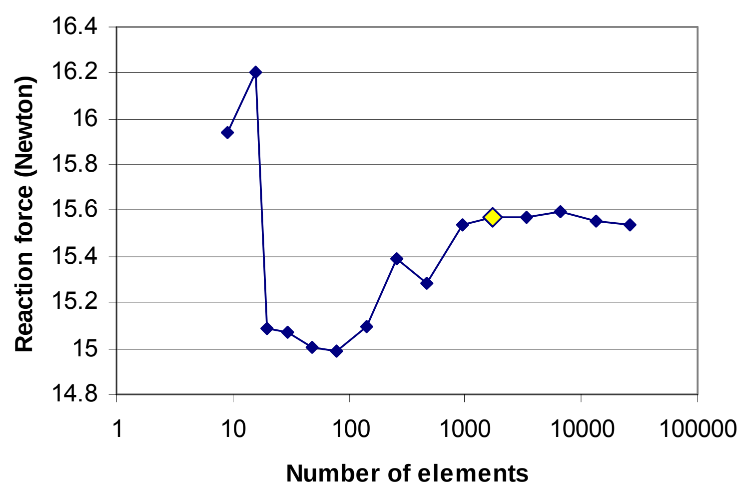

Figure 3: Convergence study to determine the number of elements

Furthermore, the model validation is performed by comparing the calculated and experimentally observed behaviours of the composite under two loading modes: (a) simple loading in tension and 3-point bending, to ensure the proper modeling of the laminate structure and its constituents, and (b) complex loading of the flexible extrados made of the same material, connected to the rigid wing structure, and deformed by two sets of locally applied actuation forces (figure 2).

3 COMPOSITE MATERIAL MANUFACTURING, CONSITUENTS AND STRUCTURE

3-1 Manufacturing

All laminates created for this study were formed through *Vacuum Assisted Resin Transfer Molding* **(**VARTM), a process which uses a vacuum to infuse resin into the reinforcement. It provides appropriate and repeatable mechanical properties, and allows the possibility of creating complex shapes. VARTM produces lower VOC (volatile organic compound) emissions than traditional vacuum bagging, while having lower set-up costs as compared to autoclave-process prepreg systems.

Testing was undertaken first to ensure the quality of the process. Matrix burnoff measurements were also conducted according to ASTM D 3171 [6]. The coefficient of variation of the fibre content was found to be smaller than 3% for all specimens tested.

3-2 Plies - constituents and characterization

Two different plies are selected to form the extrados laminate, and are presented in figure 4. The 2 x 2 twill woven Kevlar/Carbon fibre hybrid is used in the chord-wise direction, where flexibility is needed for profile modification. The low-modulus unidirectional carbon fibre is used span-wise, in which case rigidity is preferred in order to ensure profile uniformity (see figure 2). A Huntsman 8602 Reninfusion low-viscosity epoxy resin system is used. This polymer matrix is well adapted to the VARTM process due to its low viscosity of 175 cP. However, this does not compromise its cured mechanical properties, as is confirmed by the mechanical testing of the laminate.

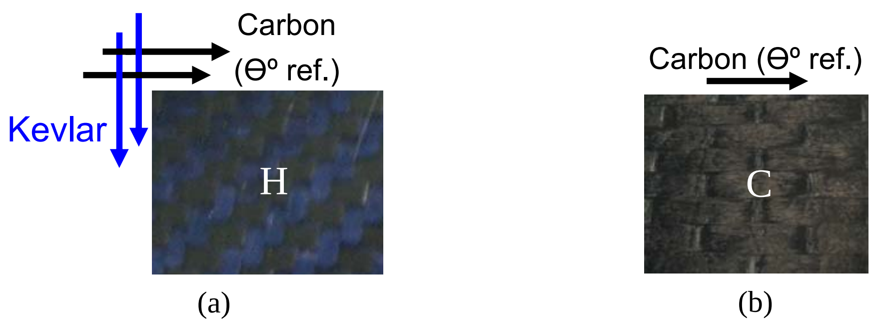

Figure 4. (a) 2x2 twill woven Kevlar/Carbon fibre hybrid (H); (b) Unidirectional carbon fibre

To calibrate the finite-elements model, tensile testing was successfully conducted according to ASTM3039 [7] and ASTM3518 [8] using 3 specimens for each ply type. The resulting average (Avg), standard deviation (SD) and coefficient of variation (CV) of each elastic constant are listed in table 1. Simplifications were made for other elastic constants listed in table 2, considering that they have a minor impact on the flexural response of the composite. The axis number 1 in the Carbon/Kevlar cloth is defined as the longitudinal axis of the carbon fibres.

Table 1. Measured elastic constants

	Const.	Avg [GPa]	SD [GPa]	CV (%)	Test method
Carbon/Kevlar Hybrid	E_1	32.9	0.7	2.2%	ASTM D3039
	E_2	17.1	0.3	1.7%	ASTM D3039
	Pr_{12}	0.12	0.026	22%	ASTM D3039
	G_{12}	2.1	0.031	1.5%	ASTM D3518
Unidirectional Carbon	E_1	99.9	2.3	2.3%	ASTM D3039
	E_2	5.5	0.4	7.2%	ASTM D3039
	Pr_{12}	0.25	0.03	10.4%	ASTM D3039
	G_{12}	3.2	0.1	3.7%	ASTM D3518

Table 2. Approximated elastic constants

	Const.	Value	Source
Carbon/Kevlar Hybrid	E_3	E_2	carbon
	G_{23}	G_{12}	C/K
	G_{13}	G_{12}	C/K
	PR_{23}	0,01	-
	PR_{13}	0,01	-
Unidirectional Carbon	E_3	E_2	carbon
	G_{23}	G_{12}	carbon
	G_{13}	G_{12}	carbon
	PR_{23}	0,01	-

3-3 Structure of the laminate

The 3- and 4-ply laminate structures shown in figure 5 were used for validation. Following analyses of the resulting ply thicknesses, some corrections were made in order to account for the woven/unidirectional reinforcement and mould contact interfaces.

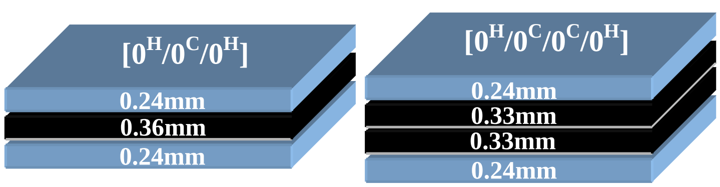

Figure 5. 3- and 4-ply laminates

4. MECHANICAL BEHAVIOUR OF THE LAMINATE UNDER SIMPLE TESTING MODES

These validation tests are aimed at verifying the ability of the models to take into account the reinforcement type, plies orientation and number.

4-1. Tensile tests

Tensile tests were performed on 3- and 4-ply laminates for three different fibre orientations (0º, 45º and 90º). The measured extensional moduli were found to be consistent with those predicted numerically, as shown in figure 6. The comparison results showed some discrepancies for the 0º and 45º orientations, and the 0º experimental modulus may have been lowered because the low 15mm coupon width amplified fibre misalignment errors.

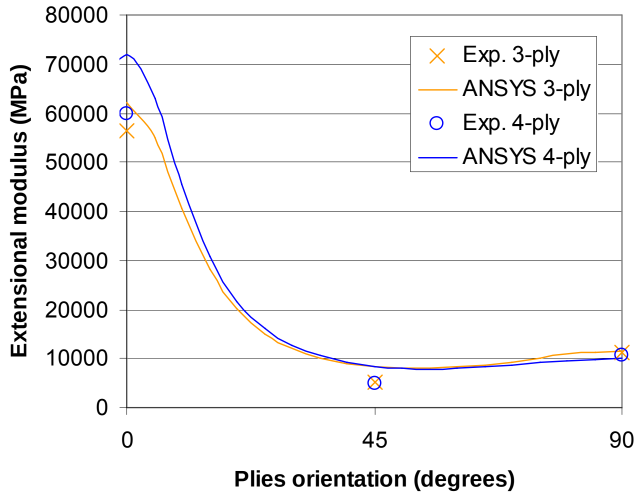

Figure 6. Laminate extensional modulus according to plies orientation and number

4-2. Three-point bending

Three-point bending is performed on the 3- and 4-ply laminates. A customized three-point bending fixture shown in figure 7, with a distance of 152.4 mm between two support lines is mounted on an MTS 858 Mini Bionix testing machine to receive 200 x 200 mm plate specimens. The load is applied by a 9.5 mm radius nose in order to avoid microbuckling fibre damage. Bending tests involving deflections of up to 10 mm are repeated for two orthogonal axes (0º and 90º), and the results are presented in figure 8 along with those predicted by the numerical model.

It can be concluded from the results obtained that the ANSYS numeric model provides good estimations of the bending stiffness for the experimental conditions tested. The bending stiffness was underestimated when the carbon fibre was solicited (0º) and overestimated when the Kevlar fibre was solicited (90º). One error source, the thickness value (t) of each ply of the laminate must be considered. In fact, the bending response (E_F) is very sensitive to the plate thickness, as the following material strength equation illustrates: $E_F = \frac{mL^3}{4bt^3}$.

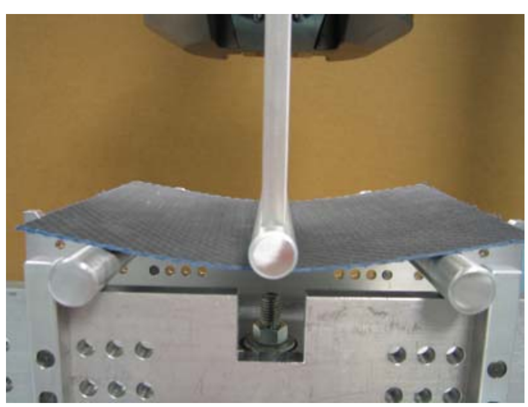

Figure 7. Three-point bending test fixture

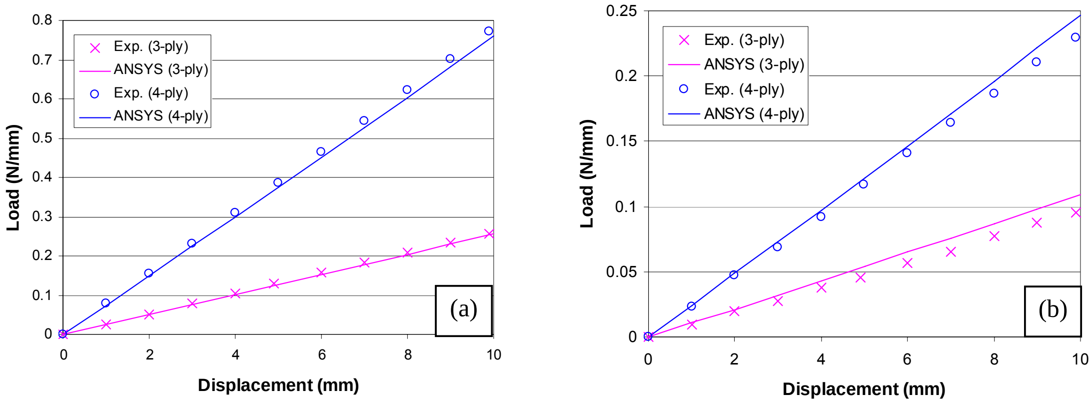

Figure 8. Normalized load deflection diagrams for (a) 0º bending direction, (b) 90º bending direction

5. MECHANICAL BEHAVIOUR OF THE FLEXIBLE EXTRADOS SUBMITTED TO ACTUATION FORCES

Given that the finite-elements model has been successfully validated for simple loading modes (tension and three-point bending), the validation is pursued by comparing numerical and experimental results of the flexible extrados submitted to actuation forces.

5-1. Laboratory testing bench for adaptive wing with flexible extrados

The adaptive-wing laboratory bench is presented in figure 9, with the profile digitizing facility located above the flexible extrados model. Using a LabView interface, a mobile laser displacement sensor measures the profile shape for a given actuation state. Both actuation lines are loaded through two actuator points for a total of four, as presented in figure 10. Deadweights are used either with or without pulleys to generate upward or downward loadings.

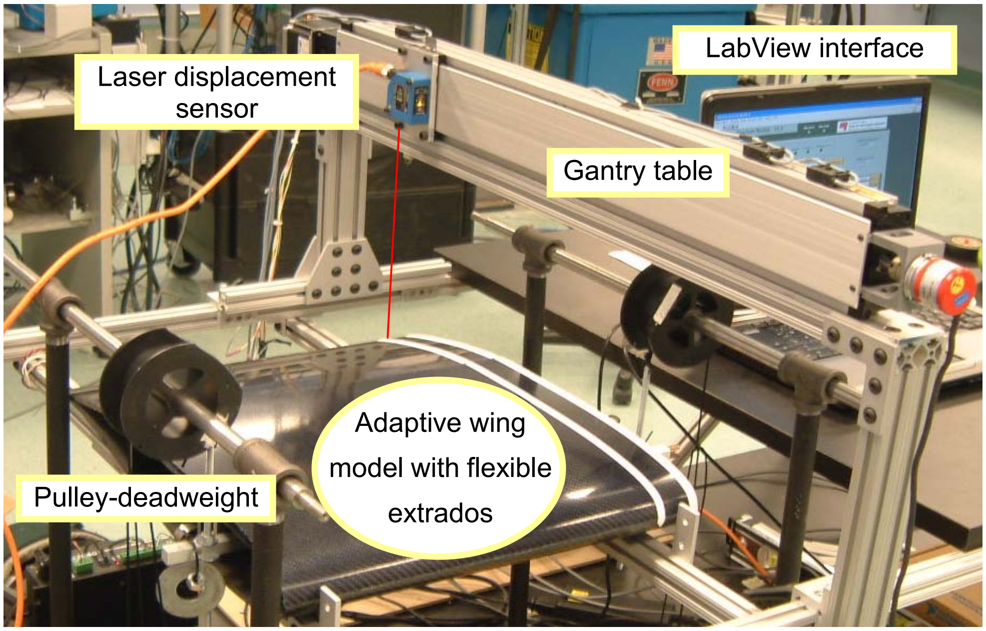

Figure 9. Adaptive wing model installed on the test bench

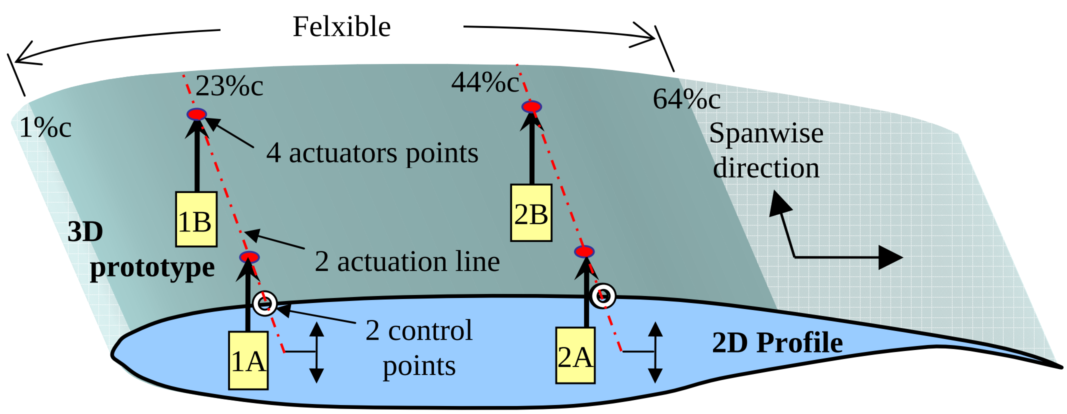

Figure 10. Wing prototype with flexible extrados

5-2. Activated extrados response

The flexible extrados uses the 3-ply laminate previously defined in figure 5, with the span direction taken to be the stacking sequence reference orientation. To gradually increase the profile thickness, the load applied at each actuation point is incremented by 2.45N from -4.9N (- signifies downward loading) to 14.7N. The load-deflection diagrams presented in figure 11 were obtained using a laser displacement sensor located directly above the actuator points. The proximity between ANSYS predictions and the experiments give confidence in the numerical model to establish functional requirements for actuators.

The respective global geometrical changes for -4.9 and 14.7 N loads were obtained when scanning the airfoil profile for the 1st and 2nd actuation lines (figure 12). For an upward deflection of over 6 mm, the difference between the calculated and the experimentally measured results did not exceed 10%. This concordance shows the ability of the numerical model to be used to design flexible wing capable of matching the theoretical profiles resulting from CFD calculations.

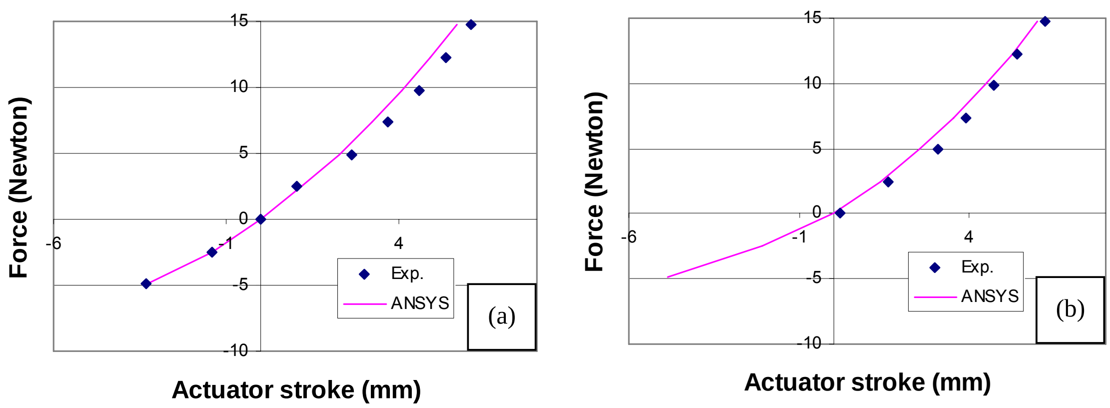

Figure 11. Load displacement diagrams: (a) 1st actuation line; (b) 2nd actuation line

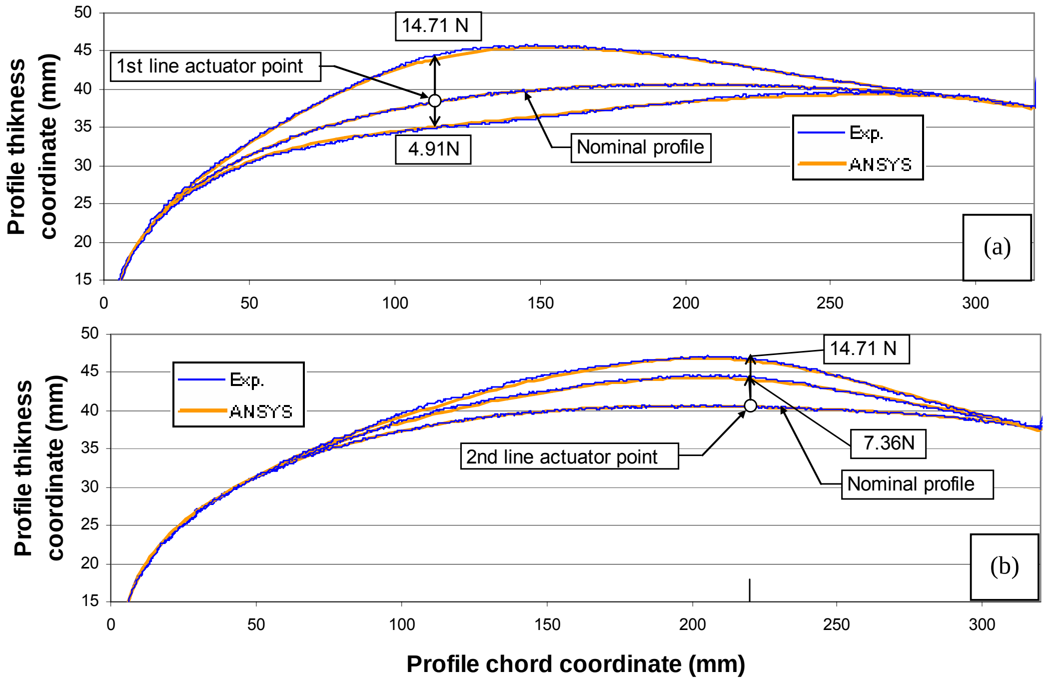

Figure 12: Experimental and computed profile shape changes for (a) 1st and (b) 2nd actuation lines

6. CONCLUSIONS

As can be seen in the experimental results, the ANSYS numerical model of the composite structure forming the flexible extrados of an adaptive wing can predict its behaviour under actuation. Using this model allows future optimization work to be conducted to optimize design variables in order to achieve specific computed wing profiles for different flow conditions, while minimizing the overall weight of the wing. To that end, a numerical tool will be developed to quantify the concordance of the shape profile obtained by mechanical modeling with that calculated through the CFD. Furthermore, aerodynamic pressure will be considered in the numerical optimization leading to an improved laminar adaptive wing. Stress distribution is another concern that will receive attention in future works in order to ensure the integrity of the whole wind tunnel prototype.

ACKNOWLEDGEMENTS

The authors would like to thank CRIAQ, NSERC, Bombardier Aerospace and Thalès Canada for their financial support as well as to acknowledge G.-H. Simon from Thalès for initiating this project and S. Rodriguez and T. Georges for their assistance in experimentations.

REFERENCES

1. Gilarranz, J.L., L.W. Traub, and O.K. Rediniotis, *A new class of synthetic jet actuators-Part II: Application to flow separation control.* Transactions of the ASME. Journal of Fluids Engineering, 2005: pp. 377-387.
2. Weissberg, V., L. Shikhmanter, and A.K. Green, *The application of shape memory alloy actuators in adaptive structures.* Proceedings of 10th International Conference on Adaptive Structures and Technologies (ICAST '99), 11-13 Oct. 1999, 2000: pp. 229-236.
3. Chandrasekhara, M.S., et al., *Design and development of a dynamically deforming leading edge airfoil for unsteady flow control.* Proceedings of the 1997 17th IEEE International Congress on Instrumentation in Aerospace Simulation Facilities, ICIASF, Sep 29-Oct 2 1997: pp. 132-140.
4. Baron A., B.B., Branchaw N., Ostry B., Pearsall J., Perlman G., Selstrom J., *Morphing Wing (MoW)*. 2003, Technical report, University of Colorado at Boulder, 102 pages.
5. Munday, D. and J. Jacob (2001), *Active control of separation on a wing with conformal camber*. Paper presented at the 39th AIAA aerospace sciences meeting and exhibit, 10 pages.
6. ASTM D3171-99, Standard Test Methods for Constituent Content of Composite Materials.
7. ASTM D3039/D3039M-00 (2006), Standard Test Method for Tensile Properties of Polymer Matrix Composite Materials.
8. ASTM D3518/D3518M-94(2001), Standard Test Method for In-Plane Shear Response of Polymer Matrix Composite Materials by Tensile Test of a ±45° Laminate.